Bol. Soc. Paran. Mat.
©SPM – E-ISSN-2175-1188
SPM: www.spm.uem.br/bspm

(3s.) **v. 2026 (44)** : 1–19.
ISSN-0037-8712
doi:10.5269/bspm.77764

# Mathematical Model of a COVID-19 Transmission in Jordan

Abdullah Abu-Rqayiq and Haneen Alayed

ABSTRACT: This paper examines the spread of the Covid-19 pandemic in Jordan, a country in the Middle East. The first recorded case dates back to March 2, 2020. During the pandemic, Jordan implemented various strategies to manage the pandemic, including lockdowns, social distancing, and school closures. In this study, we develop a fractional-order mathematical model to investigate the dynamics of the pandemic. The model is analyzed both qualitatively and numerically. Qualitatively, it reveals two equilibrium points: the Covid-19 free equilibrium and the Covid-19 endemic equilibrium. The local asymptotic stability of these equilibrium points is explored, showing a dependence on the basic reproduction number $\mathcal{R}_0$. Data from the Covid-19 dashboard of the Jordanian Ministry of Health is used to validate our model. Numerical simulations provide several typical solution paths with biological explanations.

Keywords: Mathematical model, Covid-19, Caputo's Derivative, local stability, Jordan.

## Contents



## 1. Introduction

In March 2020, the world faced a global pandemic for the first time in a century, claiming millions of lives. On March 11, 2020, the World Health Organization (WHO) declared COVID-19 a pandemic as it spread worldwide rapidly following a logistic growth pattern [1]. The virus that causes COVID-19, known as severe acute respiratory syndrome coronavirus 2 (SARS-CoV-2), spreads quickly through close contact between people. The ongoing COVID-19 pandemic spreads more efficiently than influenza but not as efficiently as highly contagious diseases like measles. Another complicating factor is that asymptomatic patients can still spread the virus. According to the Centers for Disease Control and Prevention (CDC), common symptoms include fever, chills, coughing, shortness of breath, and sore throat, among others [2].

As infected populations and death tolls continued to increase rapidly, governments around the world tried to control the pandemic by reducing close contact between people. The measures included closing public places, schools, colleges, universities, restaurants, and playgrounds. Due to the lack of proper viral

2020 *Mathematics Subject Classification:* 92D30.
Submitted July 09, 2025. Published March 22, 2026

medicine or vaccine, strategies such as travel bans from highly infected areas, social distancing, lockdown policies, isolation of infected individuals, self-quarantine of exposed individuals, mandatory use of face masks, and strictly following all social-conscious and prevention strategies were widely used to contain the virus.

Mathematical models are essential tools for analyzing and discussing infectious diseases. They aid in studying the dynamic behavior of the disease, predicting the number of cases, and determining disease transmission by finding the basic reproduction number. Additionally, they assist in deciding the best preventive measures for the situation. Many researchers have discussed COVID-19 mathematically with different models. For example, Hassan et al. conducted a prediction model analysis to determine the status of COVID-19 at the county levels in Texas [3]. Alzahrani et al. presented four prediction models to forecast the daily numbers of COVID-19 infections in Saudi Arabia [4], while Alboaneen et al. provided two models to predict the number of cases in the same region [5].

The presence of patients with asymptomatics has led investigators to focus on including this class of patients in their studies of COVID-19 [6,7]. Kim et al. [6] determined the spread of asymptomatic cases in South Korea. In their study, they found that 19% of the infected individuals with COVID-19 were asymptomatic. These results suggest applying social distancing and other restrictions to prevent the transmission of the disease through these individuals. Aljishi et al. [7] described the spread of COVID-19 at the epicenter of its spread in Saudi Arabia. The effectiveness and impact of social distancing in limiting the spread of COVID-19 were analyzed by researchers such as Al-Tuwairki and Al-Harbi [8],

On February 27, Jordan banned non-Jordanian travelers from high-risk countries from entering the country. The first COVID-19 case was reported on March 2, involving a national who had arrived from Italy. In the same week, Jordan began quarantining arrivals from selected European countries. By March 15, 12 new cases were reported, prompting the government to impose further restrictions. All educational institutions, tourism sites, cafes, and restaurants were ordered to close, and all arriving passengers were treated as suspected cases and immediately quarantined [9].

On March 2, 2020, the Jordanian government reported the first case of coronavirus in Jordan for a person who returned from Italy. [wikipedia] From March 3 to March 14, there were no new reported cases of Covid-19 in Jordan. On March 15, the government announced 12 new cases bringing the total number of positive cases to 13. On mARH 16, the number of confirmed cases rose to 29 cases. After that, the new cases were confirmed daily and by March 21, the total number of the confirmed cases was 99 including one recovery case. For the rest of March of the year 2020 the number of cases continued to rise and quarantine was applied to the confirmed cases. The total of the confirmed cases by the end of March was 274 cases and 4 new recoveries with a total of 30 confirmed recovered cases in Jordan.

By March 18, Jordan had implemented a series of stringent measures: travel between governorates was prohibited, all flights were suspended, borders were closed, public transportation was halted, commercial complexes were shut down, non-emergency medical services were suspended, and both public and private sectors were closed. A stay-at-home policy was enforced, and public, social, and religious events were prohibited. The government declared a national lockdown, a state of emergency, and imposed a curfew, mandating the wearing of face masks in public places, including cars.

During the initial days of the curfew, a complete nationwide lockdown was enforced, preventing people from leaving their homes. The citizens were later allowed five specific days to move around and walk, with neighborhood grocery stores allowed to open between 10 AM and 6 PM. Driving was not allowed, and movement between administrative geographic boundaries was only permitted under emergency circumstances.

The number of newly reported COVID-19 cases in Jordan fluctuated between three and 42 daily cases, with an average of 15 cases per day. As of May 1, 2020, the total number of reported cases was 459, including eight deaths. The cases appeared to have clustered among persons within the same family, and a limited number of cases have been identified to be of unknown origin. The test was carried out randomly, regardless of symptoms, within each of the 12 Jordanian governorates, and a limited number of cases have been identified using this approach. In early May 2020, the number of local cases reached zero for about 10 days.

In April, 2020, the number of confirmed cases increased daily and by the end of April the total number of recoveries was 453 confirmed cases and the total number of confirmed recoveries was 364 cases. In

August 2020, the restrictions were gradually eased, but confirmed cases continued to occur on a daily basis [1,9].

In November 2020, the pandemic hit the country strike. The number of confirmed cases rose dramatically and Jordan, the country that professionally responded to the pandemic, became the Arab country with the highest number of deaths related to Covid-19 per capita.

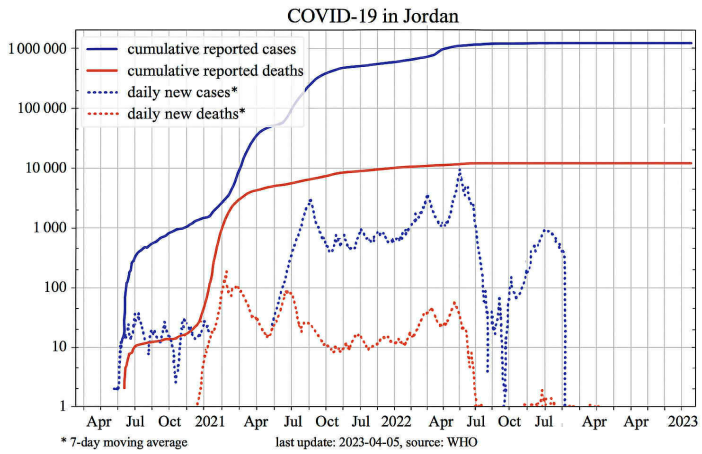


Figure 1: Number of Confirmed Cases and Deaths on a Logarithmic Scale [9].

Jordan's comprehensive response, characterized by stringent border controls and extensive testing, adhered to global best practices, leading to lower case and death rates compared to developed nations. The successful vaccination campaign, which notably ensured equitable access for refugees, significantly reduced mortality and achieved herd immunity against severe outcomes. However, the pandemic also exposed weaknesses in research and healthcare infrastructure, underscoring the urgent need for investment in virology and healthcare capacity. For more information on how to improve pandemic preparedness read [10]. Figure 1 presents the reported COVID-19 cases and deaths in Jordan on a logarithmic scale, spanning April 2020 to April 2023. The solid blue line shows cumulative confirmed cases, while the solid red line shows cumulative deaths. Dotted lines represent daily new cases and deaths (7-day moving average). This visualization highlights the major waves of infection and the overall impact of the pandemic in Jordan.

To properly understand the situation, it was essential to simulate the COVID-19 epidemic curve in Jordan, particularly for those with mild symptoms. This simulation could significantly improve public health response planning and future expectations. Furthermore, it would advance our understanding of COVID-19 in developing countries and the impact of widely supported public health measures in Jordan. The research aimed to mathematically simulate the COVID-19 outbreak in Jordan and investigate the transmission of COVID-19 in Jordan.

The development of mathematical models for COVID-19 has been a crucial aspect in understanding and managing the pandemic. These models range from simple compartmental models, such as the SIR (Susceptible-Infectious-Recovered) model, to more complex models that incorporate various factors such as age structure, spatial distribution, and intervention strategies. Among these, fractional-order models have gained attention for their ability to capture the memory and hereditary properties of the disease dynamics. Fractional-order models use derivatives of noninteger orders, providing a more accurate representation of real-world phenomena compared to integer-order models. These models have been particularly useful in describing the spread of COVID-19 and predicting the impact of different control measures. Applying a fractional derivative approach is very powerful in presenting the memory of the derivatives and the previous states of the model's compartments. The fractional approach was applied to COVID-19 models for prediction and studying the dynamics. For example, Shaikh et al. [11] applied a fractional derivative approach to simulate the potential transmission dynamics of COVID-19 in India,

Zhang et al. [12] studied the Covid-19 epidemic with isolated class. Examples of other references that use a fractional derivative approach for studying COVID-19 are [13,20].

In this paper, we formulate a fractional-order model to describe the transmission of COVID-19 in Jordan. Our model includes four compartments: susceptible, asymptomatically infected, symptomatically infected, and recovered individuals. The analysis of this model aims to study the dynamics of the outbreak in Jordan, which is crucial for current and future planning and the implementation of control measures. In addition, it helps to estimate key parameters such as the basic reproduction number, which indicates how easily the virus spreads. Understanding these parameters is essential to assess the potential impact of the virus and the effectiveness of control measures.

The rest of the article is organized as follows. Section 2 presents a summary of important preliminaries for fractional derivatives. In Section 3, we formulate the model and prove that it is well posed. In Section 4,we demonstrate the qualitative analysis, including the equilibrium points, basic and control reproduction numbers, and the local stability of the equilibrium points. In Section 5, we provide a sensitivity and numerical analysis, including the fitting of the model to the COVID-19 cases in Jordan and the estimation of the model parameters. Furthermore, we present numerical simulations that were conducted to confirm the results of the qualitative analysis and investigate the sensitivity analysis for the control reproduction number. Section 6 provides a general discussion, and Section 7 presents a conclusion of the paper.

## 2. Preliminaries

Fractional calculus, a field that extends classical derivatives and integrals to fractional orders, has a rich history dating back to Leibniz's inquiries in 1695. This branch of applied mathematics deals with real-world phenomena modeled by non-integer-order derivatives and has been gaining increasing attention globally. Fractional calculus provides a more accurate representation of complex systems and processes that exhibit memory and hereditary properties, which are often observed in various scientific and engineering applications [21].

Over the years, several types of fractional derivatives have been developed, each with unique characteristics and applications. These include the Caputo, Riemann–Liouville, Katugampola, Caputo–Fabrizio, and Atangana–Baleanu derivatives. The Caputo derivative, for instance, is widely used in modeling physical and engineering processes due to its ability to handle initial conditions in a manner similar to classical integer-order derivatives. The Riemann–Liouville derivative, on the other hand, is often employed in theoretical studies and mathematical formulations.

The Katugampola derivative introduces a generalized approach that unifies various fractional derivatives, while the Caputo–Fabrizio derivative is known for its non-singular kernel, making it suitable for modeling processes with smooth transitions. The Atangana–Baleanu derivative, with its non-local and non-singular kernel, has been particularly effective in capturing the complex dynamics of systems with long-range interactions and memory effects [22].

The applications of fractional calculus are vast and diverse, spanning fields such as physics, engineering, biology, finance, and control theory. In physics, fractional calculus is used to model anomalous diffusion and viscoelastic materials. In engineering, it helps in the design of control systems and signal processing. In biology, fractional models are employed to describe the dynamics of biological systems and population growth. In finance, fractional calculus is used to model market behavior and option pricing. Control theory benefits from fractional calculus in the development of robust and adaptive control strategies.

This section contains some preliminary definitions of fractional calculus and the associated notation. We first give the definition of fractional order integration and fractional order [21].

**Definition 2.1** *Let $L^1 = L^1[a,b]$ be the class of Lebesgue integrable functions on $[a,b]$, $a < b < \infty$. The fractional integral of order $\nu \in \mathbb{R}^+$ of the function $f(t), t > 0$ ($f : \mathbb{R}^+ \longrightarrow \mathbb{R}$) is defined by*

$$I_a^\nu = \frac{1}{\Gamma(\nu)} \int_a^t (t-s)^{\nu-1} f(s) ds, t > 0, \tag{2.1}$$

*where $\Gamma(.)$ is the Gamma function.*

The fractional derivative of order $\alpha \in (n-1, n)$ of the function $f(t)$ is defined in several ways, the most common ones are:

(i) Riemann-Liouville fractional derivative:
Take the fractional integral of order $(n-\alpha)$ and then apply the $n^{th}$ derivative

$$D_{\alpha}^{a} f(t) = D_{\alpha}^{a} I_{n-\alpha}^{a}, \tag{2.2}$$

where $D_n^* = \frac{d^n}{dt^n}, n = 1, 2, ...$

(ii) Caputo's fractional derivative:
Start with a $n^{th}$ derivative of the function, then take a fractional integral of order $(n-\alpha)$

$$D_{\alpha}^{a} f(t) = I_{n-\alpha}^{a} D_{n}^{a} f(t), n = 1, 2, ... \tag{2.3}$$

We notice that the definition of the time-fractional derivative of a function $f(t)$ at $t = t_n$ involves an integration and calculating time-fractional derivative that requires all the past history, that is, all the values of $f(t)$ from $t = 0$ to $t = t_n$. Caputo's definition, which is a modification of the Riemann-Liouville definition, has the advantage of dealing properly with initial value problems and it solves the problem of the derivative of constants.

**Definition 2.2 (The Mittag-Leffler functions)** *Two parametric Mittag-Leffler functions are represented by the series.*

$$E_{\alpha,\beta}(z) = \sum_{k=0}^{\infty} \frac{z^k}{\Gamma(\alpha k + \beta)}, \alpha, \beta > 0, \alpha, \beta \in \mathbb{R}, z \in \mathbb{C}$$

For more properties and applications of fractional derivatives and integrals, see for example [21] and [24].

## 3. Mathematical Model

Mathematical models do not offer a definitive cure for infectious diseases; rather, they serve as invaluable tools to simulate various scenarios and dynamics, assess resilience, and devise effective detection and control strategies. These models help in understanding the potential outcomes of different interventions and guide policymakers in making informed decisions. Timely and appropriate interventions are crucial for mitigating the social impact of diseases by controlling their spread. Numerous mathematical models have been proposed in the literature to understand and predict the spread of infectious diseases. The primary objectives of these models are to flatten the infection curve, reduce mortality rates, and ultimately improve public health outcomes. By simulating different intervention strategies, these models can help identify the most effective measures to contain outbreaks and minimize their impact on society [23].

Mathematical modeling plays a pivotal role in understanding and predicting the spread of COVID-19. Various types of mathematical models can be employed to simulate the spread of the virus, including compartmental models, network models, and agent-based models. Compartmental models, such as the SIR (Susceptible-Infectious-Recovered) and SEIR (Susceptible-Exposed-Infectious-Recovered) models, divide the population into different compartments based on disease status and use differential equations to describe the transitions between these compartments. Network models, on the other hand, represent individuals as nodes in a network and simulate the spread of the virus through connections between nodes, capturing the heterogeneity of contact patterns. Agent-based models simulate the actions and interactions of individual agents, allowing for a more detailed representation of the population and the spread of the virus.

By leveraging these different modeling approaches, researchers can gain a comprehensive understanding of the dynamics of COVID-19 and evaluate the effectiveness of various intervention strategies. This knowledge is crucial for developing targeted and effective public health measures to control the spread of the virus and mitigate its impact on society.

Compartmental models divide the population into different compartments, such as susceptible, infected, and recovered individuals, and use mathematical equations to describe the flow of individuals

between these compartments. These models can be used to estimate the basic reproduction number $\mathcal{R}_0$ of the virus, which is a measure of how easily it spreads, and to predict the size and timing of outbreaks.

Network models take into account the social interactions between individuals and can be used to simulate the spread of the virus in specific populations, such as schools, hospitals, or households.

Agent-based models simulate the behavior of individual agents, such as individuals or households, and their interactions with each other. These models can be used to study the impact of different interventions, such as social distancing or masking, on the spread of the virus.

In this study, we consider an SEIR-modified model with a combined compartment for exposed and asymptomatic individuals, which reduces the number of parameters in the model. The model divides the size of the population of Jordan, N, into four compartments: susceptible $S(t)$, asymptomatically infected $I_a(t)$, symptomatically infected $I_s(t)$, and recovered individuals $R(t)$ at time $t$ per day unit. Where, susceptible individuals are those who are not yet infected, asymptomatically infected individuals are those who have been infected but with no symptoms, symptomatically infected individuals (with symptoms), and recovered individuals are those who have been infected and then removed from the disease due to recovery or death. We denote by $\Lambda$ the natural birth rate, $\beta_1$ and $\beta_2$ are disease transmission rates of susceptible individuals with asymptomatically and symptomatically ones, respectively, which may cause the transmission of the infection, $\sigma$ is the transition rate from $I_a$ to $I_s$ compartments, $\mu_1$ and $\mu_2$ are the natural death rate and disease (due to Covid-19) death rate and $\delta$ is the recovery rate. Note that the parameters $\beta_1^\alpha I_a$ and $\beta_2^\alpha I_s$ represent the force of virus infection. We assume that individuals in the asymptomatic compartment can transmit the disease more than individuals in the symptomatic compartment, that is, $\beta_2 > \beta_1$. The model is described by the following system of nonlinear fractional ordinary differential equations:

$$\begin{aligned} D_t^\alpha S &= \Lambda - (\beta_1 I_a + \beta_2 I_s + \mu_1)S \\ D_t^\alpha I_a &= (\beta_1 I_a + \beta_2 I_s)S - (\sigma + \gamma + \mu_1)I_a \\ D_t^\alpha I_s &= \sigma I_a - (\gamma + \mu_1 + \mu_2)I_s \\ D_t^\alpha R &= \gamma I_a + \gamma I_s - \mu_1 R, \end{aligned} \tag{3.1}$$

where $D_t^\alpha$ is the Caputo fractional derivative and $0 < \alpha \leq 1$. The initial values assumed in the model (3.1) are:

$$S(0) \geq 0, I_a(0) \geq 0, I_s(0) \geq 0, \text{and} \quad R(0) \geq 0$$

In the next Theorem, we prove that the positive invariant domain of system (3.1) is

$$D = \{(S, I_a, I_s, R) \in \mathbb{R}_+^4 : 0 \leq N \leq \frac{\Lambda}{\mu_1}\},$$

where $N = S + I_a + I_s + R$.

This is a biologically meaningful range of variables. Figure 2 shows the compartmental diagram for model (3.1).

**Theorem 3.1** *Considering model (3.1) assumptions, all solutions of the system are positive and bounded in the invariance region with nonnegative initial conditions in the region*

$$D = \{(S, I_a, I_s, R) \in \mathbb{R}_+^4 : 0 \leq N \leq \frac{\Lambda}{\mu_1}\}.$$

**Proof:** First, we show that all solutions are positive. Let $(S(0), I_a(0), I_s(0), R(0)) \in D$. We have

$$\begin{aligned} D_t^\alpha S(t) &= \Lambda \geq 0, \\ D_t^\alpha I_a(t) &= \beta_2 I_s(t) S(t) \geq 0, \\ D_t^\alpha I_s(t) &= \sigma I_a \geq 0, \\ D_t^\alpha R(t) &= \gamma(I_a(t) + I_s(t)) \geq 0. \end{aligned}$$

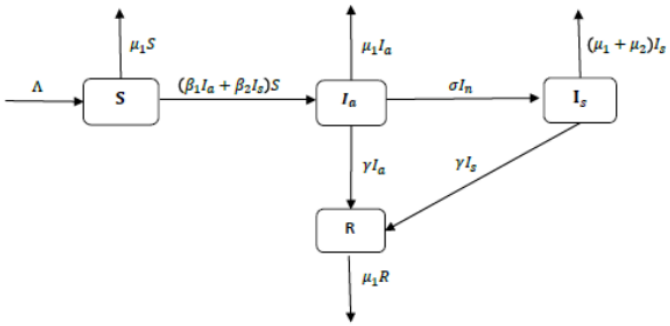


Figure 2: Compartmental diagram for the model

Table 1: Pameters' Description

| Parameter | Description | Value | Unit | Source |
|---|---|---|---|---|
| $N$ | Total population in Jordan | $10.806 \times 10^6$ | individual | [9] |
| $\Lambda$ | Birth rate | 395 | $individual \times day^{-1}$ | [9] |
| $\sigma$ | Transition rate from $I_a$ to $I_s$ | 0.167 | $day^{-1}$ | Estimated |
| $\gamma$ | Recovery rate | 0.5 | $day^{-1}$ | Estimated |
| $\beta_1$ | Transmission rate by $I_a$ | $1.059 \times 10^{-7}$ | $individual \times day^{-1}$ | Estimated |
| $\beta_2$ | Transmission rate by $I_s$ | $0.0554 \times 10^{-7}$ | $individual \times day^{-1}$ | Estimated |
| $\mu_1$ | Natural death rate | $3.6529 \times 10^{-5}$ | $day^{-1}$ | [9] |
| $\mu_2$ | Death rate due to Covid-19 | $1.2907 \times 10^{-2}$ | $day^{-1}$ | [9] |

Thus, for $t \geq 0$ all positive solutions remain positive. Next, combining all equations of (3.1), we get

$$D_t^\alpha = \Lambda - \mu_2 I_s - \mu_1 N \leq \Lambda - \mu_1 N,$$

where $N = S + I_a + I_s + R$. Using the integrating factor technique for the above fractional differential inequality, we get

$$N(t) \leq N(0)E_\alpha(-\mu_1 t^\alpha) + \frac{\Lambda}{\mu_1}(1 - E_\alpha(-\mu_1 t^\alpha)),$$

Where $E_\alpha(t) = \sum_{k=0}^{\infty} \frac{t^k}{\Gamma(k\alpha+1)}$ is the Mittag Leffler function.
Thus,

$$\limsup_{t \longrightarrow \infty} \leq \frac{\Lambda}{\mu_1}. \tag{3.2}$$

Hence, all solutions of model (3.1) are bounded and non-negative for all $t \geq 0$. Therefore, the domain $D$ is positively invariant. □

Next, we prove the existence and uniquness for the solution to the system (3.1).

**Lemma 3.1** *Consider the system* ${}_{t_0}^{C}D_t^a \mathrm{x(t)} = \mathrm{g(t,x)}, \mathrm{t_0} > 0$, *with initial condition* $\mathrm{x\,(t_0)} = \mathrm{x_{t_0}}$, *where,* $\alpha \in (0,1], \mathrm{g} : [\mathrm{t_0}, \infty) \times \Omega \to \mathbb{R}, \Omega \subseteq \mathrm{C}^1\,[t_0, \infty)$, *if local Lipschitz condition is satisfied by* $g(t,x)$ *with respect to* $x$, *then there exists a unique solution on* $[\mathrm{t_0}, \infty) \times \Omega$.

**Theorem 3.2** *(Existence and Uniqueness) For any time t, the solution of system (3.1) will exist and the solution will be unique.*

**Proof:** Consider the region $\Omega \times [t_0, \gamma]$, where

$$\Omega = \left\{(S, I_a, I_s, R) \in \mathbb{R}^4, S, I_a, I_s, R \in C^1[t_0, \infty) \wedge \|S\|, \|I_a\|, \|I_s\|, \|R\| \leq M\right\} \quad \text{and} \quad \gamma < \infty.$$

Let $K(S) = \Lambda - (\beta_1 I_a + \beta_2 I_s + \mu_1)S$,

$$\begin{aligned}
&\|K(S_1) - K(S_2)\| = \|\Lambda - (\beta_1 I_a + \beta_2 I_s + \mu_1)S_1 - \Lambda + (\beta_1 I_a + \beta_2 I_s + \mu_1)S_2\|, \\
&= \|\beta_1 I_a(S_2 - S_1) + \beta_2 I_s(S_2 - S_1) + (S_2 - S_1)\mu_1\|, \\
&\leq \beta_1 \|I_a\| \|S_2 - S_1\| + \beta_2 \|I_s\| \|S_2 - S_1\| + \mu_1 \|S_2 - S_1\|, \\
&= (\beta_1 \|I_a\| + \beta_2 \|I_s\| + \mu_1) \|S_2 - S_1\|, \\
&\leq (\beta_1 + \beta_2 + \mu_1) M \|S_2 - S_1\|.
\end{aligned}$$

Thus,

$$\|K(S_1) - K(S_2)\| \leq (\beta_1 + \beta_2 + \mu_1) M \|S_2 - S_1\|$$

Therefore, $K(S)$ satisfies Lipschitz condition.

Let $L(S) = (\beta_1 I_a + \beta_2 I_s)S - (\sigma + \gamma + \mu_1)I_a$,

$$\begin{aligned}
&\|L(I_{a_1}) - L(I_{a_2})\| = \|(\beta_1 I_{a_1} + \beta_2 I_s)S - (\sigma + \gamma + \mu_1)I_{a_1} - (\beta_1 I_{a_2} + \beta_2 I_s)S + (\sigma + \gamma + \mu_1)I_{a_2}\|, \\
&= \|\beta_1 S(I_{a_1} - I_{a_2}) + (\sigma + \gamma + \mu_1)(I_{a_1} - I_{a_2})\|, \\
&\leq \beta_1 \|S\| \|I_{a_1} - I_{a_2}\| + (\sigma + \gamma + \mu_1) \|I_{a_1} - I_{a_2}\|, \\
&\leq (\beta_1 \|S\| + \sigma + \gamma + \mu_1) \|I_{a_1} - I_{a_2}\| \\
&\leq (\beta_1 M + \sigma + \gamma + \mu_1) \|I_{a_1} - I_{a_2}\|.
\end{aligned}$$

Thus,

$$\|L(I_{a_1}) - L(I_{a_2})\| \leq (\beta_1 M + \sigma + \gamma + \mu_1) \|I_{a_1} - I_{a_2}\|$$

Therefore, $L(S)$ satisfies Lipschitz condition.

Let $N(I_{a_s}) = \sigma I_a - (\gamma + \mu_1 + \mu_2)I_s$,

$$\begin{aligned}
&\|N(I_{s_1}) - N(I_{s_2})\| = \|(\sigma I_a - (\gamma + \mu_1 + \mu_2)I_{s_1} - \sigma I_a + (\gamma + \mu_1 + \mu_2)I_{s_2}\| \\
&\leq (\gamma + \mu_1 + \mu_2) \|N(I_{s_1}) - N(I_{s_2})\|
\end{aligned}$$

Thus,

$$\|N(I_{s_1}) - N(I_{s_2})\| \leq (\gamma + \mu_1 + \mu_2) \|N(I_{s_1}) - N(I_{s_2})\|$$

Therefore, $N(S)$ satisfies Lipschitz condition.

□

Let $P(R) = \gamma I_a + \gamma I_s - \mu_1 R$,

$$\begin{aligned}
&\|P(R_1) - P(R_1)\| = \|\gamma I_a + \gamma I_s - \mu_1 R_1 - \gamma I_a - \gamma I_s + \mu_1 R_2\| \\
&= \|\mu_1(R_2 - R_1)\|, \\
&\leq \|(R_1 - R_2\|
\end{aligned}$$

Since $\mu_1 < 1$. Therefore, $P(R)$ satisfies the Lipschitz condition.
Let, $F_1 = (\beta_1 + \beta_2 + \mu_1) M, F_2 = (\beta_1 M + \sigma + \gamma + \mu_1), F_3 = (\gamma + \mu_1 + \mu_2), F_4 = \mu_1^{\alpha}$.
Also, let $F = \max\{F_1, F_2, F_3, F_4\}$. Therefore,

$$\begin{aligned}
\|K(S_1) - K(S_2)\| &\leq F \|S_1 - S_2\| \\
\|L(I_{a_1}) - L(I_{a_2})\| &\leq F \|I_{a_1} - I_{a_2}\| \\
\|N(I_{s_1}) - N(I_{s_2})\| &\leq F \|I_{s_1} - I_{s_2}\| \\
\|P(R_1) - P(R_2)\| &\leq F \|R_1 - R_2\|
\end{aligned}$$

For $F < 1$, $K(S), L(I_a), N(I_s)$, and $P(R)$ are contraction mappings.
Therefore, according to the Banach fixed point Theorem, the solution to system (3.1) exists and is unique.

## 4. Equilibria and Stability

In this section, we describe the qualitative behavior of the model (3.1). We determine equilibrium points and the basic reproduction number. We also investigate the local and global stability of the equilibrium points.

### 4.1. Equilibrium Points and basic reproduction number

To Find the equilibrium points of the model (3.1), we set fractional derivatives equal to zero.

$$D_t^\alpha S = 0,\ D_t^\alpha I_a = 0,\ D_t^\alpha I_s = 0, \text{ and } D_t^\alpha R = 0,$$

and we write,

$$\begin{aligned}
\Lambda - (\beta_1 I_a + \beta_2 I_s + \mu_1)S &= 0,\\
(\beta_1 I_a + \beta_2 I_s)S - (\sigma + \gamma + \mu_1)I_a &= 0,\\
\sigma I_a - (\gamma + \mu_1 + \mu_2)I_s &= 0,\\
\gamma I_a + \gamma I_s - \mu_1 R &= 0.
\end{aligned}$$

The analytic solution of system (3.1) yields two equilibrium points in the domain $D$: The Covid-19 free disease equilibrium point (DFE) $E_0 = (\frac{\Lambda}{\mu_1}, 0, 0, 0)$ that always exists and typically occurs when assuming that $I_a = 0$ and $I_s = 0$, and the Covid-19 endemic equilibrium point $E* = (S^*, I_a^*, I_s^*, R^*)$, where

$$\begin{aligned}
S^* &= \frac{\Lambda}{\mu_1 \mathcal{R}_0},\\
I_a^* &= \frac{\Lambda \mathcal{R}_0}{\mathcal{R}_0(\sigma + \gamma + \mu_1) + 1},\\
I_s^* &= \frac{\Lambda \sigma \mathcal{R}_0}{\mathcal{R}_0(\sigma + \gamma + \mu_1)(\gamma + \mu_1 + \mu_2) + (\gamma + \mu_1 + \mu_2)},\\
R^* &= \frac{\gamma \Lambda \mathcal{R}_0(\gamma + \mu_1 + \mu_2 + \sigma))}{\mu_1(\gamma + \mu_1 + \mu_2)(\mathcal{R}_0(\sigma + \gamma + \mu_1) + 1)}.
\end{aligned}$$

Here, $\mathcal{R}_0 = \frac{\Lambda\beta_1(\mu_1+\mu_2+\gamma)+\Lambda\beta_2\sigma}{\mu_1(\mu_1+\sigma+\gamma)(\mu_1+\mu_2+\gamma)}$. The endemic equilibrium point $E^*$ exists only if $\mathcal{R}_0 > 1$.

**Basic Reproduction Number:**

The basic reproduction number denoted $\mathcal{R}_0$, can be considered as the number of secondary cases of infection generated from a single virus in a population where all tumor cells are susceptible to infection. Applying the Next Generation Method [25]. Let $\mathcal{P} = (S, I_a, I_s, R)$, then model (3.1) can be rewritten as $\mathcal{P}' = \tilde{F}(\mathcal{P}) - \tilde{V}(\mathcal{P})$, where the matrices $\tilde{F}$ and $\tilde{V}$ represent respective new infection and transition, and they are given by

$$\tilde{F}(\mathcal{P}) = \begin{pmatrix} \beta_1 S_0 & \beta_2 S_0 \\ 0 & 0 \end{pmatrix},$$

and

$$\tilde{V}(\mathcal{P}) = \begin{pmatrix} \sigma + \gamma + \mu_1 & 0 \\ -\sigma & \gamma + \mu_1 + \mu_2 \end{pmatrix}$$

Therefore, the $V^{-1}$ matrix is

$$\tilde{V^{-1}}(\mathcal{P}) = \begin{pmatrix} \frac{1}{\sigma+\gamma+\mu_1} & 0 \\ \frac{\sigma}{(\sigma+\gamma+\mu_1)(\mu_1+\mu_2+\gamma)} & \frac{1}{\gamma+\mu_1+\mu_2} \end{pmatrix}$$

Thus, the next-generation matrix $FV^{-1}$ is

$$F\tilde{V}^{-1}(\mathcal{P}) = \begin{pmatrix} \frac{\beta_1(\gamma+\mu_1+\mu_2)S_0+\beta_2\sigma S_0}{(\sigma+\gamma+\mu_1)(\gamma+\mu_1+\mu_2)} & \frac{\beta_2 S_0}{\gamma+\mu_1+\mu_2} \\ 0 & 0 \end{pmatrix}$$

Hence, the basic production number $\mathcal{R}_0 = \rho(FV^{-1}) = \frac{\beta_1(\gamma+\mu_1+\mu_2)S_0+\beta_2\sigma S_0}{(\sigma+\gamma+\mu_1)(\gamma+\mu_1+\mu_2)}$

### 4.2. Local Stability Analysis

We employ the linearization method [26] to investigate the stability of the equilibrium points of Model (3.1).

**Theorem 4.1** *For the system (3.1), the Covid-19 free equilibrium point $E_0$ is locally asymptotically stable if $\mathcal{R}_0 < 1$, and unstable otherwise.*

**Proof:**

The Jacobian matrix evaluated at the Covid-19 free equilibrium point is given by

$$J(E_0) = \begin{pmatrix} -\mu_1 & -\beta_1 S_0 & -\beta_2 S_0 & 0 \\ 0 & \beta_1 S_0 - (\sigma+\gamma+\mu_1) & \beta_2 S_0 & 0 \\ 0 & \sigma & -(\gamma+\mu_1+\mu_2) & 0 \\ 0 & \gamma & \gamma & -\mu_1 \end{pmatrix}$$

By solving the characteristic equation $|J(E_0) - \lambda I| = 0$, we obtain four eigenvalues as follows: $\lambda_1 = -\mu_1$, $\lambda_2 = \beta_1 S_0 - (\sigma+\gamma+\mu_1),$, $-(\gamma+\mu_1+\mu_2)$, and $\lambda_4 = -\mu_1$.

$$P(\lambda) = \lambda^2 + a_1\lambda + a_2 = 0, \tag{4.1}$$

where

$$a_1 = \sigma + 2\gamma + \mu_1 + 2\mu_1 + \mu_2) - \beta_1 S_0,$$

and

$$a_2 = (\gamma+\mu_1+\mu_2)(\sigma+\gamma+\mu_1-\beta_1 S_0) - \beta_2\sigma S_0$$

$$= (\sigma+\gamma+\mu_1)(\gamma+\mu_1+\mu_2)(1 - \frac{\beta_1(\gamma+\mu_1+\mu_2)S_0+\beta_2\sigma S_0}{(\sigma+\gamma+\mu_1)(\gamma+\mu_1+\mu_2)})$$
$$= (\sigma+\gamma+\mu_1)(\gamma+\mu_1+\mu_2)(1-\mathcal{R}_0)$$

Using Routh-Hurwitz criteria [26], the roots of equation (4.1) are negative if $a_1 > 0$ and $a_2 > 0$. This happens when $\mathcal{R}_0 < 1$. It is obvious that $a_2 > 0$ if $\mathcal{R}_0 < 1$. However, it is not obvious that $a_1 > 0$. To show this, $\mathcal{R}_0 < 1$ implies that

$$\frac{\beta_1(\gamma_2+\mu_1+\mu_2)S_0+\beta_2\sigma S_0}{(\sigma+\gamma_1+\mu_1)(\gamma_2+\mu_1+\mu_2)} < 1$$
$$\frac{\beta_1 S_0}{\sigma+\gamma_1+\mu_1} + \frac{\beta_2\sigma S_0}{(\sigma+\gamma_1+\mu_1)(\gamma_2+\mu_1+\mu_2)} < 1$$
$$\beta_1 S_0 + \frac{\beta_2\sigma S_0}{\gamma_2+\mu_1+\mu_2} < \sigma+\gamma_1+\mu_1$$
$$\frac{\beta_2\sigma S_0}{\gamma_2+\mu_1+\mu_2} < (\sigma+\gamma_1+\mu_1) - \beta_1 S_0$$
$$\frac{\beta_2\sigma S_0}{\gamma_2+\mu_1+\mu_2} + (\gamma_2+\mu_1+\mu_2) < (\sigma+\gamma_1+\mu_1) + (\gamma_2+\mu_1+\mu_2) - \beta_1 S_0$$

Which implies that, $0 < \frac{\beta_2\sigma S_0}{\gamma_2+\mu_1+\mu_2} + (\gamma_2+\mu_1+\mu_2) < a_1$. Thus, $a_1 > 0$ and the Routh-Hurwitz criterion for polynomials implies that the DFE is stable.

If $\mathcal{R}_0 > 1$, then $a_2 < 0$. Thus, $P(0) = B < 0$. Again, $P(\lambda) \to \infty$ as $\lambda \to \infty$. Since $P(\lambda)$ is a continuous function of $\lambda$, hence by Bolzano's theorem on continuous function we have $P(\lambda_i) = 0$ for some $\lambda_i > 0$. Therefore, at least one eigenvalue of the Jacobian matrix is positive. Hence, DFE point is unstable equilibrium point [3]. □

**Theorem 4.2** *For the system (3.1), the Covid-19 endemic equilibrium point $E*$ is locally asymptotically stable if $\mathcal{R}_0 > 1$, and unstable otherwise.*

**Proof:** The Jacobian matrix evaluated at $E^*$ is given by

$$J(E^*) = \begin{pmatrix} -(\beta_1 I_a^* + \beta_2 I_s^*) - \mu_1) & -\beta_1 & -\beta_2 & 0 \\ \beta_1 I_a^* + \beta_2 I_s^* & \beta_1 - (\sigma + \gamma + \mu_1) & \beta_2 & 0 \\ 0 & \sigma & -(\gamma + \mu_1 + \mu_2) & 0 \\ 0 & \gamma & \gamma & -\mu_1 \end{pmatrix}$$

Solving the characteristic equation $|J(E^* - \lambda I| = 0$ yields $\lambda_1 = \mu_1$ which is negative, and the remaining eigenvalues are the roots of the equation

$$\lambda^3 + a_1\lambda^2 + a_2\lambda + a_3 = 0, \tag{4.2}$$

where

$$\begin{aligned}
a_1 &= \sigma + 2\gamma + 3\mu_1 + \mu_2 + \beta_1 I_a^* + \beta_2 I_s^* - \beta_1 S^* \\
a_2 &= -2\gamma\beta_1 I_a^* - 2\mu_1\beta_1 I_a^* - \sigma\beta_2 I_s^* - 2\mu_1\beta_2 I_s^* + 2\mu_1\beta_1 S^* - 2\sigma\mu_1 - 3\gamma\mu_1 - 3\mu_1^2 + \gamma\beta_1 S^* + \beta_1\mu_2 \\
&\quad - S^* - \sigma\gamma - \sigma\mu_2 - \gamma^2 - \gamma\mu_2 - 2\mu_1\mu_2 - \beta_1\mu_2 I_a^* - \beta_2\mu_2 I_s^* - \gamma\mu_1 \\
a_3 &= -\beta_1\gamma\sigma I_a^* - \beta_1\gamma^2 I_a^* - 2\beta_1\gamma\mu_1 I_a^* - \beta_2\gamma\sigma I_s^* - \beta_2\gamma^2 I_s^* - 2\beta_2\gamma\mu_1 I_s^* + \beta_1\gamma\mu_1 S^* - \gamma\sigma\mu_1 - \gamma^2\mu_1 \\
&\quad - \gamma\mu_1 - \beta_1\sigma\mu_1 I_a^* - \beta_1\mu_1^2 I_a^* - \beta_2\sigma\mu_1 I_s^* - \beta_2\mu_1^2 I_s^* + \beta_1\mu_1^2 S^* - \sigma\mu_1^2 - \gamma\mu_1^2 - \mu_1^3 - \beta_1\sigma\mu_2 I_a^* - \\
&\quad \gamma\beta_1\mu_2 I_a^* - \beta_1\mu_1\mu_2 I_a^* - \beta_2\sigma\mu_2 I_s^* - \beta_2\gamma\mu_2 I_s^* - \beta_2\mu_1\mu_2 I_s^* + \beta_1\mu_1\mu_2 S^* - \sigma\mu_1\mu_2 - \gamma\mu_1\mu_2 - \mu_1\mu_2 \\
&\quad - \beta_1\beta_2\sigma S^* I_a^* - \beta_2^2\sigma S^* I_a^*.
\end{aligned}$$

We use the Routh-Hurwitz criteria to determine the sign of the remaining eigenvalues. The first eigenvalue is negative, then the system will be locally asymptotically stable if other 3 eigenvalues are all negative or their real parts are negative. The other three eigenvalues will be negative or will have negative real parts if the Routh-Hurwitz criterion is satisfied. From Routh-Hurwitz criterion, we can say that the EE point is stable if $a_1 > 0$, $a_3 > 0$ and $a_1 a_2 > a_3$. Therefore the EE ,which exists if $\mathcal{R}_0 > 1$, is locally asymptotically stable. □

## 5. Numerical Analysis

In this section, we fit model (3.1) to the actual data of Covid-19 cases in Jordan and estimates the parameters that make it compatible with reality. We provide sensitivity analysis of the model, and then we provide a numerical analysis with simulations.

### 5.1. Sensitivity Analysis

Here, we conduct a sensitivity analysis on our model to determine parameters that have a high impact on the threshold $\mathcal{R}_O$ and should be targeted by intervention strategies. this analysis allows us to measure the relative change in a variable when a parameter changes. However, sensitivity has the drawback that it does not give the change of quantity $\mathcal{R}_0$ relative to the size of the quantity. To address this problem, the elasticity of the reproduction number $\mathcal{R}_0$ can be used and defined as follows

$$\mathcal{E}^p_{\mathcal{R}_O} = \frac{\partial \mathcal{R}_0}{\partial p}\frac{p}{\mathcal{R}_0},$$

where $p$ is a parameter [25]. The magnitude of the elasticity indices generally depends on the parameter values found in the expression of $\mathcal{R}_0$.

In our analysis of the sensitivity of the basic reproductive number $\mathcal{R}_0$, we evaluated the impact of various parameters on $\mathcal{R}_0$. The parameters analyzed included are $\Lambda, \beta_1, \beta_2, \gamma, \mu_1, \mu_2$, and $\sigma$. Our findings indicate that $\Lambda$ and $\mu_1$ are the most influential parameters, with sensitivity indices of 1 and $-1$, as shown in Table 2, respectively. This implies that a 1% increase in $\Lambda$ will result in a 1% increase in $\mathcal{R}_0$, while a 1%

increase in $\mu_1$ will lead to a 1% decrease in $\mathcal{R}_0$. Similarly, $\beta_1$ has a significant positive influence, with a sensitivity index of 0.9830, indicating that a 1% increase in $\beta_1$ will cause $\mathcal{R}_0$ to increase by approximately 0.9832%. Conversely, $\gamma$ and $\sigma$ have negative sensitivity indices of $-0.9845$ and $-0.2340$, respectively, suggesting that a 1% increase in $\gamma$ will decrease $\mathcal{R}_0$ by 0.9840%, and a 1% increase in $\sigma$ will decrease $\mathcal{R}_0$ by 0.2340%. The parameters $\beta_2$ and $\mu_2$ have relatively smaller influences, with sensitivity indices of 0.0167 and $-0.0004$, respectively. These results highlight the critical parameters that should be targeted in interventions to control the spread of infectious diseases.

The models indicate that the most critical parameters are $\beta_1$ and $\gamma$, with sensitivity indices of 0.9830

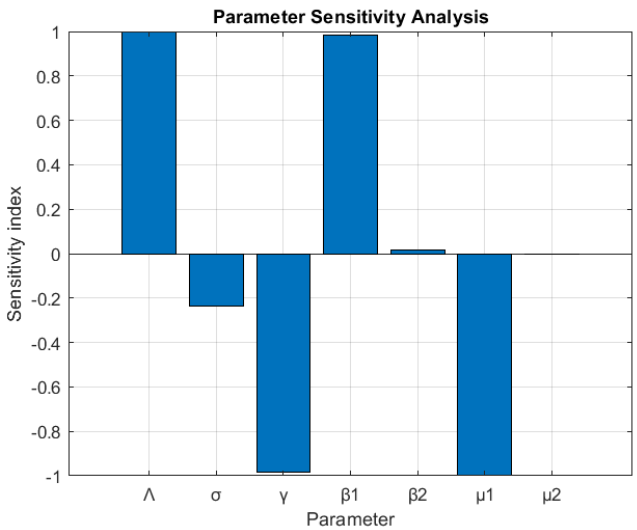


Figure 3: Bar chart shows sensitivity index for each parameter

and $-0.9845$, respectively. Figure 3 displays a bar chart of sensitivity indices for key model parameters affecting the basic reproduction number $\mathcal{R}_0$. Parameters such as the birth rate ($\Lambda$), transmission rates ($\beta_1$and $\beta_2$), recovery rate ($\gamma$), and death rates ($\mu_1$ and $\mu_2$) are shown. The chart illustrates which parameters most strongly influence $\mathcal{R}_0$, guiding intervention strategies. Controlling the outbreak effectively could involve managing these parameters. Since $\beta_1$ represents the transmission rate from the susceptible (S) to the asymptomatic infected ($I_a$) class through contact with $I_a$ individuals, reducing contact between asymptomatic individuals and the general population is crucial. One proven measure is the uniform use of face masks by all populations, which significantly reduces contact between classes and, consequently, disease transmission. Additionally, if doctors can develop an effective antiviral medication to improve the recovery rate, it could serve as another effective method to control the disease.

The rate of change of $\mathcal{R}_0$ with respect to one parameter at a time is given as follows:

$$\frac{\partial \mathcal{R}_0}{\partial \Lambda} = \frac{\beta_1(\gamma+\mu_1+\mu_2)+\beta_2\sigma}{\mu_1(\sigma+\gamma+\mu_1)(\gamma+\mu_1+\mu_2)} > 0,$$
$$\frac{\partial \mathcal{R}_0}{\partial \beta_1} = \frac{\Lambda}{\mu_1(\sigma+\gamma+\mu_1)} > 0,$$
$$\frac{\partial \mathcal{R}_0}{\partial \beta_2} = \frac{\Lambda\sigma}{\mu_1(\sigma+\gamma+\mu_1)(\gamma+\mu_1+\mu_2)} > 0,$$
$$\frac{\partial \mathcal{R}_0}{\partial \mu_1} = -\frac{\Lambda(\sigma+\gamma+2\mu_1)}{\mu_1^2(\sigma+\gamma+\mu_1)}\left[\frac{\beta_1}{\gamma+\mu_1+\mu_2}+\frac{\beta_2\sigma}{(\gamma+\mu_1+\mu_2)^2}\right]-\frac{\Lambda\beta_2\sigma}{\mu_1(\sigma+\gamma+\mu_1)(\gamma+\mu_1+\mu_2)^2} < 0,$$
$$\frac{\partial \mathcal{R}_0}{\partial \mu_2} = -\frac{\beta_2\sigma\Lambda}{\mu_1(\gamma+\mu_1+\mu_2)^2(\sigma+\gamma+\mu_1)} < 0,$$
$$\frac{\partial \mathcal{R}_0}{\partial \gamma} = -\frac{\beta_1\mu_1\Lambda}{\mu_1^2(\sigma+\gamma+\mu_1)^2}-\frac{\beta_2\sigma\Lambda}{(\sigma+\gamma+\mu)^2} < 0,$$
$$\frac{\partial \mathcal{R}_0}{\partial \sigma} = \frac{\Lambda}{\mu_1(\sigma+\gamma+\mu_1)^2)(\gamma+\mu_1+\mu_2)}[\beta_2(\gamma+\mu_1)-\beta_1(\gamma+\mu_1+\mu_2)] > 0.$$

The above equations show that $\mathcal{R}_0$ decreases when $\mu_1$, $\mu_2$, and $\gamma$ increase. In contrast, $\mathcal{R}_0$ increases when $\Lambda$, $\beta_1$, $\beta_2$, and $\sigma$ increase.

Now we compute the elasticity index of $\mathcal{E}^p_{\mathcal{R}_O}$ with respect to the model parameter $p$.

$$\mathcal{E}^{\Lambda}_{\mathcal{R}_0} = \frac{\partial \mathcal{R}_0}{\partial \Lambda}\frac{\Lambda}{\mathcal{R}_0} = 1,$$
$$\mathcal{E}^{\beta_1}_{\mathcal{R}_O} = \frac{\partial \mathcal{R}_0}{\partial \beta_1}\frac{\beta_1}{\mathcal{R}_0} = \frac{\beta_1(\gamma+\mu_1+\mu_2)}{\beta_1(\gamma+\mu_1+\mu_2)+\beta_2\sigma},$$
$$\mathcal{E}^{\beta_2}_{\mathcal{R}_O} = \frac{\partial \mathcal{R}_0}{\partial \beta_2}\frac{\beta_2}{\mathcal{R}_0} = \frac{\beta_2\sigma}{\beta_1(\gamma+\mu_1+\mu_2)+\beta_2\sigma},$$
$$\mathcal{E}^{\mu_1}_{\mathcal{R}_O} = \frac{\partial \mathcal{R}_0}{\partial \mu_1}\frac{\mu_1}{\mathcal{R}_0} = \frac{\beta_1\mu_1}{\beta_1(\gamma+\mu_1+\mu_2)+\beta_2\sigma}-\frac{\mu_1(\sigma+\gamma+\mu_1)+(\gamma+\mu_1+\mu_2)(2\mu_1+\sigma+\gamma)}{(\sigma+\gamma+\mu_1)(\gamma+\mu_1+\mu_2)},$$
$$\mathcal{E}^{\mu_2}_{\mathcal{R}_O} = \frac{\partial \mathcal{R}_0}{\partial \mu_2}\frac{\mu_2}{\mathcal{R}_0} = \frac{\beta_1\mu_2}{\beta_1(\gamma+\mu_1+\mu_2)+\beta_2\sigma}-\frac{\mu_2}{\gamma+\mu_1+\mu_2},$$
$$\mathcal{E}^{\gamma}_{\mathcal{R}_0} = \frac{\partial \mathcal{R}_0}{\partial \gamma}\frac{\gamma}{\mathcal{R}_0} = \frac{\beta_1\gamma}{\beta_1(\sigma+\gamma+\mu_1)+\beta_2\sigma}-\frac{\gamma(\sigma+2\gamma+2\mu_1+\mu_2)}{(\sigma+\gamma+\mu_1)(\gamma+\mu_1+\mu_2)},$$
$$\mathcal{E}^{\sigma}_{\mathcal{R}_O} = \frac{\partial \mathcal{R}_0}{\partial \sigma}\frac{\sigma}{\mathcal{R}_0} = \frac{\sigma\beta_2}{\beta_1(\gamma+\mu_1+\mu_2)+\beta_2\sigma}-\frac{\sigma}{\mu_1+\sigma+\gamma}.$$

The mathematical model (3.1) describes the dynamics of Covid-19 and is validated by fitting the model with existing pandemic data. We use data from the official Jordanian Ministry of Health website [9]. We consider the active cases of Covid-19 from March 2,2020, to December 31, 2020, where at this time interval the Jordanian government applied different levels of lockdown, social distancing, and vaccination. These different levels of action have been applied almost since the early cases were recorded. Therefore, we did not incorporate those parameters that can describe the government's actions since the measures can vary widely during the pandemic times. For instance, the Jordanian government applied lockdown on some days and allowed for one day weekly with no lockdown, then it changes the times of lockdown as the pandemic curve changed. Vaccinations also varied hugely as most of the population hesitated to take them at the beginning, but then it started to grow. Social distancing also was not luckier as people changed their attitudes about Covid-19 hugely during the pandemic. Therefore, we did not incorporate those parameters in order to introduce a more general and more accurate model that can describe the

Table 2: Sensitivity index for $\mathcal{R}_0$ with respect to the parameters $\mathcal{P}$ of model (3.1)

| Parameter $\mathcal{P}$ | Value | Sensitivity index $\mathcal{E}^{\mathcal{P}}_{\mathcal{R}_0}$ |
|---|---|---|
| $\Lambda$ | 395 | 1 |
| $\sigma$ | 0.167 | -0.2340 |
| $\gamma$ | 0.5 | -0.9845 |
| $\beta_1$ | $1.059 \times 10^{-7}$ | 0.9830 |
| $\beta_2$ | $0.0554 \times 10^{-7}$ | 0.0167 |
| $\mu_1$ | $3.6529 \times 10^{-5}$ | -1 |
| $\mu_2$ | $1.2907 \times 10^{-2}$ | -0.0004 |

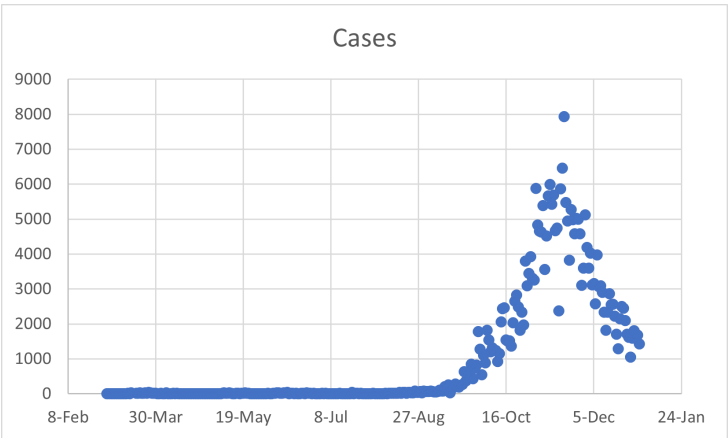


Figure 4: Scatter plot that shows the distribution of COVID-19 cases in 2020

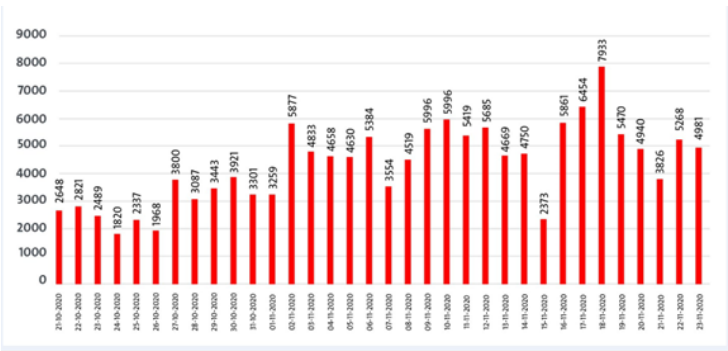


Figure 5: The chart shows the recorded cases from October 21, 2020, to November 23, 2020
The maximum number of recorded daily cases was recorded on November 18 and it was 7933 cases.

pandemic mathematically. It is worth mentioning that this is the first complete mathematical-based study on Covid-19 in Jordan.

### 5.2. Model Fitting and Estimation of Parameters

We estimate the parameters of model (3.1) to validate it with the actual data of Covid-19 infected cases in Jordan. We use the available data on the COVID-19 database of the Jordan Ministry of Health to validate our model. We consider the active cases of COVID-19 from March 2, 2020, till December 31, 2020. Figur 5 illustrates the daily recorded cases and deaths in Jordan from October 21, 2020, to

November 23, 2020. The top panel shows daily cases, with a peak of 7,933 cases on November 18. The bottom panel shows daily deaths, reflecting the severity of the pandemic during this period. We estimate the parameters: $\beta_1$, $\beta_2$, $\sigma$, and $\Lambda$ as given in Table 1, which is similar to those in [3] and [8]. The remaining parameters are obtained from the Jordanian Ministry of Health [9].

The natural death rate, $\mu_1$, is estimated as follows:

$$\mu_1 = \frac{1}{75 \times 365} = 3.6529 \times 10^{-5} \text{ per day.}$$

Since $N(t) \approx \frac{\Lambda}{\mu_1}$, Assuming that the population in the absence of disease is $N(0) = \frac{\Lambda}{\mu_1}$, we estimate the birth rate $\Lambda = 395$. Here $N(0) = 10,806,000$, the total Jordan population in 2019. Figure 4 provides a scatter plot showing the distribution of COVID-19 cases in Jordan during 2020. The plot visualizes the daily case counts, highlighting the initial outbreak and subsequent waves throughout the year.

The incubation period (the transition rate from $I_a$ to $I_s$) is the period of disease development that represents the transition rate from asymptomatically infected to infected compartment. In Jordan, this period is estimated to be 6 days. Hence, we need the parameter $\sigma$ to have a value of $\frac{1}{6}$ or 0.167.

### 5.3. Numerical Simulations

We perform simulations for model (3.1) with different initial values. We aim to show the consistency between the numerical solutions and the qualitative analysis discussed in this paper. The values of the initial conditions are chosen from the set: $\Omega = \{(S, I_a, I_s, R) : 0 < S + I_a + I_s + R \leq 1\}$.

In this numerical analysis, we employ the Caputo-fractional derivative to demonstrate the dependency of solutions on all preceding states. We select three appropriate values for the order of the fractional derivative: $\alpha = 1$, which corresponds to the conventional first derivative, and $\alpha = 0.9$ and $\alpha = 0.8$, to illustrate the inherent memory effect of the fractional derivative.

To solve the system of fractional differential equations numerically, we use Matlab. The code used in the simulations implements the predictor-corrector method proposed by Diethelm and Freed in [27], with the stability properties of this method discussed in [28]. The model parameters are chosen to satisfy the stability conditions for each equilibrium in the qualitative analysis. The numerical simulations reveal that the solution curves approach $E_0$ if $\mathcal{R}_0 < 1$ and $E^*$ if $\mathcal{R}_0 > 1$.

Let us first re-scale the state variables in the model. Let

$$S = \overline{S}N, I_a = \overline{I_a}N, I_s = \overline{I_s}N, R = \overline{R}N$$

Substituting this in model (3.1) and removing the bars over variables we get:

$$\begin{aligned}
D_t^\alpha S &= \mu_1 - (\beta_1 I_a + \beta_2 I_s)\frac{\Lambda}{\mu_1} S - \mu_1 S \\
D_t^\alpha I_a &= (\beta_1 I_a + \beta_2 I_s)\frac{\Lambda}{\mu_1} S - (\sigma + \gamma + \mu_1) I_a \\
D_t^\alpha I_s &= \sigma I_a - (\gamma + \mu + \mu_2) I_s \\
D_t^\alpha R &= \gamma I_a + \gamma I_s - \mu_1 R
\end{aligned}$$

Here, we have used $N = \frac{\Lambda}{\mu_1}$. We solve the system numerically using the following initial conditions:

$$S(0) = 0.8, I_a(0) = 0.1, I_s(0) = 0.05, R(0) = 0.01$$

The initial conditions are chosen from the set $\Omega = \{(S, I_a, I_s, R) : 0 \leq S + I_a + I_s + R \leq 1\}$. The parameters are chosen to satisfy the stability conditions for each equilibrium point.

To perform the numerical simulations, we chose the following values for the parameters of model (3.1). Let $\Lambda = 395, \sigma = 0.167, \gamma = 3.2772 * 10^{-1}, \beta_1 = 1.059 * 10^{-7}, \beta_2 = 0.0554 * 10^{-7}, \mu_1 = 0.04$, and $\mu_2 = 1.2907 * 10^{-2}$. Here, $\mathcal{R}_0 = 0.002 < 1$. In this case, the solution curves of the module will approach

the COVID-19 free equilibrium point $E_0 = (1, 0, 0, 0)$. This can be observed in Figure 6, which shows the stability of the equilibrium point. Note that here we increased the value of the parameter $\mu_1$ to obtain stable solutions.
Then, we increase the parameters $\mu_1$ and $\beta_1$. So, the parameter values are: $\Lambda = 395, \sigma = 0.167, \gamma = 0.7, \beta_1 = 1.059 * 10^{-4}, \beta_2 = 0.0554 * 10^{-7}, \mu_1 = 0.04$, and $\mu_2 = 1.089 * 10^{-5}$. Here, $\mathcal{R}_0 = 1.956 > 1$. In this case, the solution curves approach the endemic equilibrium point

$$E^* = (0.502985, 0.03774518, 0.0165672, 0.43116).$$

This is shown in Figure 7.

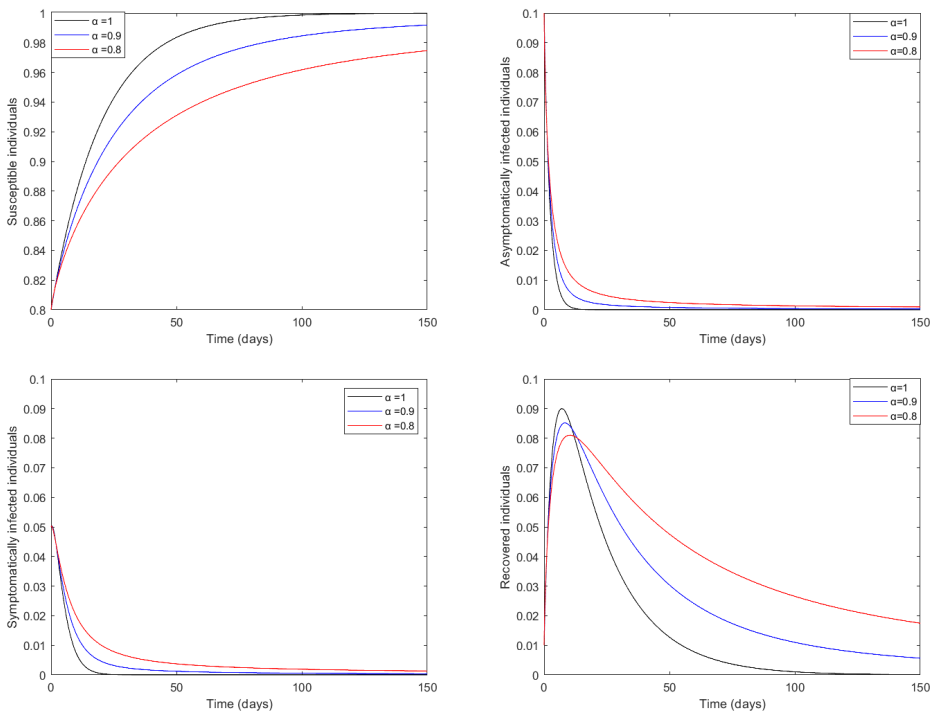


Figure 6: Dynamics of the model with initial values $S = 0.8$, $I_a = 0.1$, $I_s = 0.05$, and $R = 0.01$ and for appropriate values of $\alpha$. This figure shows that $E_0$ is asymptotically stable for $\mathcal{R}_0 < 1$.

From the above numerical analysis, we conclude that the numerical results agree with the qualitative results.

## 6. Discussion

The COVID-19 pandemic, declared in March 2020, marked the most significant global public health crisis since the 1918 influenza outbreak. Like many countries, Jordan responded with a combination of swift policy interventions and evolving social behaviors. The first case in Jordan was reported on March 2, 2020, and in the weeks that followed, the country implemented aggressive non-pharmaceutical interventions (NPIs), including curfews, school closures, travel bans, and public gathering restrictions. These actions had a visible impact on the progression of the disease, but as the year progressed, the epidemic curve in Jordan experienced multiple phases, including a prolonged plateau and a sharp rise in the fall of 2020. To understand and simulate such complex behavior, mathematical models became essential tools in guiding public health policy and forecasting future trends [29].

In this study, we developed and analyzed a fractional-order $SI_aI_sR$ model to simulate the dynamics of COVID-19 transmission in Jordan. The model incorporates the Caputo fractional derivative, which allows the system to capture memory effects—representing the influence of prior states on current dynamics.

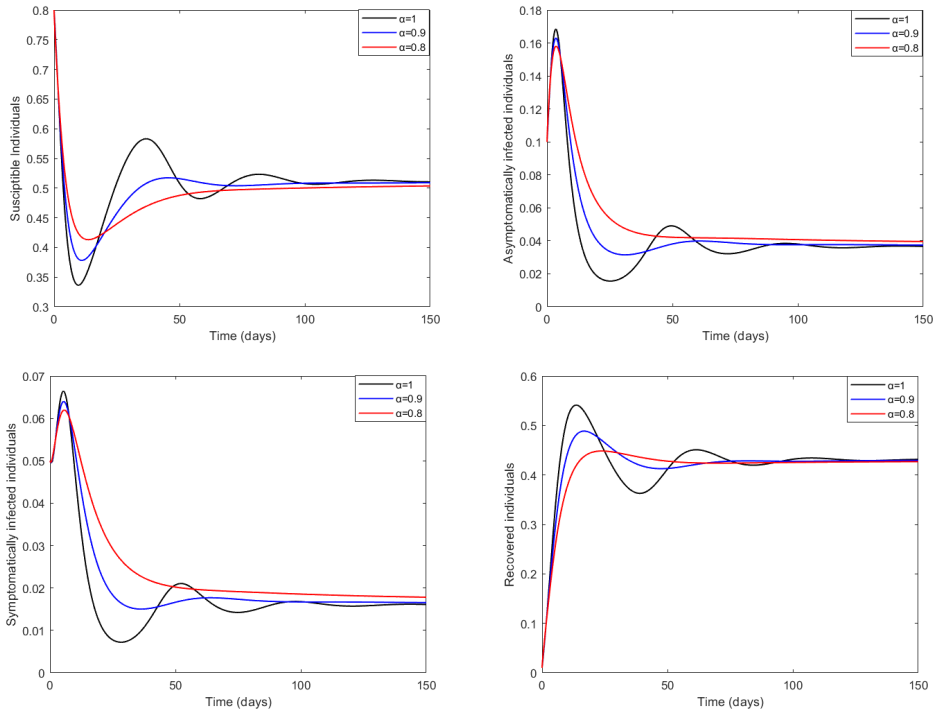


Figure 7: Dynamics of the model with initial values $S = 0.8$, $I_a = 0.1$, $I_s = 0.05$, and $R = 0.01$ and for appropriate values of $\alpha$. This figure shows that $E^*$ is asymptotically stable for $\mathcal{R}_0 > 1$.

This is especially important in modeling infectious diseases, where the transmission dynamics are not only a function of the present moment but also shaped by past exposures, delayed policy responses, and behavioral adaptation. Our numerical simulations with varying values of the fractional order $\alpha$ demonstrated that smaller $\alpha$ values correspond to slower epidemic dynamics, which is consistent with the idea of lingering effects from prior states. Conversely, when $\alpha$ approaches 1, the system behaves more like a traditional integer-order model, with faster transmission and recovery dynamics. These results show that the fractional model provides a more realistic and flexible framework for modeling real-world disease dynamics, particularly in a context like Jordan, where public response and policy measures shifted over time.

The sensitivity analysis further revealed key parameters that most significantly affect the basic reproduction number $\mathcal{R}_0$, which governs whether an epidemic grows or dies out. Among these, the natural birth rate $\Lambda$ and the natural death rate $\mu_1$ had the strongest influence, with sensitivity indices of $+1$ and $-1$ respectively. This means that small changes in these demographic rates directly impact $\mathcal{R}_0$ in a proportional way. More notably, the transmission rate from asymptomatic individuals $\beta_1$ emerged as a critical driver of disease spread—approximately five times more impactful than the corresponding rate from symptomatic individuals $\beta_2$. This finding reflects one of the most important characteristics of COVID-19: its capacity to spread silently through individuals who do not display symptoms but remain infectious. In practical terms, this insight emphasizes the importance of interventions that can curb hidden transmission, such as mass testing, mask mandates, and improved ventilation.

Another key parameter in the model is the recovery rate $\gamma$, which was shown to significantly suppress the reproduction number. An increase in $\gamma$, whether through clinical care improvements, pharmaceutical interventions, or effective vaccination campaigns, has a nearly one-to-one negative impact on $\mathcal{R}_0$. This suggests that even modest improvements in patient recovery speed can have meaningful effects on disease containment. The numerical simulations aligned with these conclusions: when the parameter set produces $\mathcal{R}_0 < 1$, the system tends toward a disease-free equilibrium, while scenarios with $\mathcal{R}_0 > 1$ exhibit convergence toward an endemic state. Additionally, changes in the fractional order $\alpha$ influence

how quickly these equilibrium states are approached. For example, higher $\alpha$ values accelerate the decline in active cases, indicating a faster rate of recovery and shorter epidemic duration, while lower $\alpha$ values reflect persistent, drawn-out dynamics.

While the model successfully captures key aspects of COVID-19 spread in Jordan, it does make certain simplifying assumptions. For example, it does not explicitly model vaccination, even though vaccination campaigns began in Jordan in late 2020. Similarly, we did not include age stratification, geographic heterogeneity, or contact networks—all of which can affect transmission patterns. These limitations were intentional in order to preserve the mathematical tractability and clarity of the fractional model. However, they also present opportunities for future research. Extending the model to include vaccination, waning immunity, and spatial mobility would further increase its relevance and predictive power, particularly as new variants continue to emerge and influence transmission dynamics.

This study offers a significant contribution by applying a fractional-order differential approach to simulate COVID-19 transmission in Jordan and studying the Covid-19 dynamics. The combination of theoretical analysis, parameter sensitivity, and numerical validation based on real-world data provides a rigorous foundation for understanding the spread of infectious diseases in a dynamic social context. It also demonstrates the value of fractional models for capturing complex temporal dependencies that are often overlooked in traditional epidemiological models. As such, this work not only contributes to the literature on COVID-19 modeling but also provides a framework that can be adapted to future outbreaks and different geographic settings.

## 7. conclusion

Our fractional derivative S$I_a I_s$R model was successfully applied to model the COVID-19 pandemic in Jordan. The fractional derivative helps to capture the memory of the state, making the model more realistic. The model can describe the dynamics of the coronavirus in Jordan and predict peaks outside the time window used to describe the basic dynamics. The use of the fractional derivative shows how the solution is continuously dependent on all previous states. The model was validated by using the data from the COVID-19 dashboard of the Jordanian Ministry of Health spanning March 2, 2020 to December 31, 2020. In addition, the numerical experiments performed using the model showed the consistency of the numerical solutions with the qualitative analysis. Under the conditions described in Theorem 1 and Theorem 2, and considering the appropriate parameter values, it is evident that the disease-free case can be attained in a real scenario. Local analysis proved that stability can be established for different values of the basic reproduction number, namely $\mathcal{R}_0 < 1$ and $\mathcal{R}_0 > 1$, and the fractional COVID-19 system preserves stability in both steady states.

## References


1. World Health Organization, https://www.who.int/Docs/Defaultsource/Coronaviruse/Who-China-Jointmission-on-Covid-19-Fnal-Report.Pd

2. Centers for Disease Control and Prevention, https://www.cdc.gov/covid/prevention/index.html

3. Hassan MN, Mahmud MS, Nipa KF, Kamrujjaman M., *Mathematical modeling and COVID-19 forecast in Texas, USA: a prediction model analysis and the probability of disease outbreak*. Disaster Med Public Health Prep. doi: https://doi.org/10.1017/dmp.(2021).151.

4. Alzahrani S., Aljamaan i., and Al-Fakih E.,*Forecasting the spread of the COVID-19 pandemic in Saudi Arabia using ARIMA prediction model under current public health interventions*, Journal of Infection and Public Health Volume 13, Issue 7, (2020), Pages 914-919

5. Alboaneen, D., Pranggono, B., Alshammari, D., Alqahtani, N., & Alyaffer, R. *Predicting the Epidemiological Outbreak of the Coronavirus Disease 2019 (Covid-19) In Saudi Arabia*. International Journal of Environmental Research and Public Health, 17(12).(2020)

6. G. Kim, M. Kim, S. Ra, J. Lee, S. Bae, J. Jung, et al., *Clinical characteristics of asymptomatic and symptomatic patients with mild COVID-19*, Clin. Microbiol. Infect., 26 (2020), 948.e1–948.e3. https://doi.org/10.1016/j.cmi.2020.04.040

7. J. M. AlJishi, A. H. Alhajjaj, F. L. Alkhabbaz, T. H. AlAbduljabar, A. Alsaif, H. Alsaif, et al., *Clinical characteristics of asymptomatic and symptomatic COVID-19 patients in the eastern province of Saudi Arabia*, J. Infect. Public Health, 14 (2021), 6–11. https://doi.org/10.1016/j.jiph.2020.11.002

8. Al-Tuwairqi S. & Al-Harbi S., *Modeling the effect of random diagnoses on the spread of COVID-19 in Saudi Arabia* Math Biosci Eng. 2022 Jul 8;19(10):9792-9824. doi: 10.3934/mbe.2022456.

9. Jordanian Ministery of Health, https://corona.moh.gov.jo

10. Hajjo R., Sabbah D., Bardaweel S., and Abusara O., *Epidemiology Analysis of COVID-19 Data and Associated Effects of Pandemic Containment Procedures, Viral Variants, and Vaccines: Lessons Learned From Middle Eastern Jordan's Experience*, Wiley, Advances in Public Health, Volume 2024, Article ID 2977631, https://doi.org/10.1155/adph/2977631

11. Shaikh, A.S., Shaikh, I.N. & Nisar, K.S., textitA mathematical model of COVID-19 using fractional derivative: outbreak in India with dynamics of transmission and contro. Adv Differ Equ 2020, 373 (2020). https://doi.org/10.1186/s13662-020-02834-3

12. Zhang, Z., Zeb, A., Egbelowo, O.F. et al., *Dynamics of a fractional order mathematical model for COVID-19 epidemic.* Adv Differ Equ 2020, 420 (2020). https://doi.org/10.1186/s13662-020-02873-w

13. Saleem S., Rafiq M., Ahmed N., Arif M., Raza A., Iqbal Z., Niazai S., and Khan I., *Fractional Epidemic Model of Coronavirus Disease with Vaccination and Crowding Effects*, Scientific Reports, (2024)

14. Baba, I. A. & Nasidi, B. A. *Fractional order epidemic model for the dynamics of novel COVID-19*, Alex. Eng. J. 60, 537–548. https://doi.org/10.1016/j.aej.2020.09.029 (2021).

15. Rajagopal, K. et al. *A fractional-order model for the novel coronavirus (COVID-19) outbreak*, Nonlinear Dyn. 101, 711–718. https://doi.org/10.1007/s11071-020-05757-6 (2020).

16. Naveed, M. et al. *Mathematical analysis of novel coronavirus (2019-NCov) delay pandemic model*, Comput. Mater. Contin. 64, 1401–1414. https://doi.org/10.32604/cmc.2020.011314 (2020).

17. Das, M. & Samanta, G. P. *Optimal control of fractional order COVID-19 epidemic spreading in Japan and India 2020*, Biophys. Rev. Lett. 15, 207–236. https://doi.org/10.1142/s179304802050006x (2020).

18. Kahn, R. et al. *Mathematical modeling to inform vaccination strategies and testing approaches for coronavirus disease 2019 (COVID-19) in nursing homes*, Clin. Infect. Dis. 74, 597–603. https://doi.org/10.1093/cid/ciab517 (2022).

19. Jiang, S. et al. *Mathematical models for devising the optimal SARS-CoV-2 strategy for eradication in China, South Korea, and Italy*, J. Transl. Med. https://doi.org/10.1186/s12967-020-02513-7 (2020).

20. Ameen, I. G., Ali, H. M., Alharthi, M. R., Abdel-Aty, A. H. & Elshehabey, H. M. *Investigation of the dynamics of COVID-19 with a fractional mathematical model: A comparative study with actual data*, Results Phys. https://doi.org/10.1016/j.rinp.2021.103976 (2021).

21. Pdlubny, I., *Fractional Differential Equations*, 1st Edition, Volume 198, (1998)

22. Syam, M. and Al-Refai M., *Fractional Differential Equations with Atangana-Baleanu Fractional Derivative: Analysis and Applications*, Chaos, Solitons & Fractals:X, Volume 2, (2019)

23. Mackenzie, D. *What's Happening in the Mathematical Sciences*, American Mathematical Society AMS, Vol 12, (2022)

24. Ray, S. et al. *Fractional calculus and its applications in applied mathematics and other sciences*. Math. Probl. Eng. 2014, 2–4 (2014).

25. Martcheva, M., *An Introduction to Mathematical Epidemiology*, Springer, New York, (2015).

26. Perko, L., *Differential Equations and Dynamical Systems*, Springer, 2001.

27. K. Diethelm and A.D. Freed, The Frac PECE subroutine for numerical solution of differential equations of fractional order, in: Forschung und Wissenschaftliches Rechnen, 1999(1999), 57-71.

28. K. Diethelm and N.J. Freed, Analysis of fractional differential equations, J. Math. Anal. Appl., 265 (2002), 229-248.

29. Mackenzie, D., *What's Hapenning in the Mathematical Scienceses*, American Mathematical Society (AMS), **12, (2022)**



*Abdullah Abu-Rqayiq,*
*Department of Mathematics,*
*University of Cincinnati,*
*Ohio, USA.*
*E-mail address:* aburqaah@ucmail.uc.edu